J Mater Sci (2009) 44:6629–6636
DOI 10.1007/s10853-009-3580-y

MESOSTRUCTURED MATERIALS

Mesoporous silica-aluminas derived from precipitation: a study of the acidity, textural properties and catalytic performance

M. Bartoszek · R. Eckelt · Ch. Jäger · H. Kosslick · A. Pawlik · A. Schulz

Received: 21 November 2008 / Accepted: 12 May 2009 / Published online: 2 June 2009

Abstract Silica-alumina covering broad range of compositions have been obtained by combined hydrolysis precipitation. These materials were characterized mainly by solid-state NMR spectroscopy. Textural properties were investigated by measurements of nitrogen sorption, and the acidity of Brønsted sites was studied by TPD and FTIR spectroscopy using ammonia as probe molecule. The catalytic performance of these materials was studied by the Brønsted acid-catalyzed acetalization reaction. New insights into the nature of the silicate compartment and the acidity of Brønsted sites of amorphous silica-alumina have been obtained. Silica-aluminas of different silica content do not represent a homologous row. They differ mainly in the connectivity of the silicate compartment. The results show that silica-alumina contain a quantitative amount of Brønsted sites. The appearance of tetrahedral Al is closely related to silica. The concentration of tetrahedral Al, and hence Brønsted acid sites, follows a volcano shape. After increasing with SiO_2 content, the site concentration reaches a maximum at 20 wt% of silica and decreases again due to the marked decrease in the total alumina content in high silica samples. Surprisingly, the catalytic activity does not follow this trend. It increases especially with high silica samples due to the interplay of acid site concentration and the strength of acid sites. The aluminosilicate compartment of high silica samples shows a high Si/Al ratio. The improved acid strength of the sites overcompensates the lower site concentration, leading to a distinctly enhanced catalytic activity.

M. Bartoszek · R. Eckelt · H. Kosslick (✉) · A. Schulz
Leibniz-Institute for Catalysis e. V, Albert-Einstein-Str. 29a, 18059 Rostock, Germany
e-mail: hendrik.kosslick@catalysis.de

H. Kosslick · A. Schulz
Institute of Chemistry, University of Rostock, Albert-Einstein-Str. 3a, 18059 Rostock, Germany

Ch. Jäger · A. Pawlik
BAM – Federal Institute for Materials Research and Testing, Division I.3, Working Group NMR Spectroscopy, Richard – Willstaetter Str. 11, 12489 Berlin, Germany

Ch. Jäger
e-mail: christian.jaeger@bam.de

Introduction

Mesoporous silica-aluminas are an important class of materials. They are widely applied in different areas such as adsorption, as catalysts or catalyst supports for hydrogenation, hydrocracking, or isomerization. Their properties, especially Brønsted acidity, are mainly determined by the content and connectivity of the silicon network as well as the state of incorporated aluminum. Despite their practical importance, comparative little scientific attention is paid to these materials [1–5].

Conducted FTIR investigations hardly show the presence of acidic hydroxyl groups. For OH vibrations, sometimes an increased absorbance is observed between 3700 and 3500 cm^{-1}. However, often no well-resolved bands of a Brønsted acidic bridging OH group could be unequivocally identified. Shifts in the stretching modes of adsorbed CO give some evidence for the presence of acidity in silica-aluminas [6–8]. High-resolution proton NMR was applied to study activated amorphous silica-aluminas and showed new possibilities to characterize surface OH groups [9].

Research efforts with silica-aluminas are presently directed to control the surface active sites. However, the experimental results obtained by various groups with

respect to the catalytic activity of sol–gel silica-aluminas, having similar compositions, differ significantly. Only general trends are similar. One open problem concerns the homogeneity of materials [10, 11].

The preparation of silica-aluminas with improved textural and acidic properties is still a challenge. This requires a better understanding of the nature of active phases related to Brønsted acidity. This article deals with the study of the nature of the silicate compartment and the formation of tetrahedral aluminum which is associated with acidic bridging OH groups in silica-aluminas. The influence of the silica content on the texture, structure, acidity, and catalytic properties is studied in detail. The influence of the Brønsted acidity on the catalytic performance has been tested by means of the acetalization of benzaldehyde with butanediol-1,3 in the liquid phase.

It will be shown that silica-aluminas of various silica contents do not represent a homologous row. They differ mainly in the nature of the silicate species, especially their connectivity. The formation of tetrahedral-coordinated aluminum species is closely related to the incorporation of silica. They show Brønsted acidity, and the corresponding catalytic activity is due to the presence of tetrahedral aluminum in the silicate phase. The catalytic activity of samples is driven by the interplay of the concentration and strength of active sites.

Experimental

Materials

Silica-alumina of different silicon to aluminum content are obtained by the hydrolysis and precipitation of organic aluminum and silicon precursors. The silicon content in the solid varied between 1 and 70 wt%. Prior to use, the samples were dried at 150 °C and re-hydrated by standing over a saturated ammonium chloride solution.

Methods

AES

The chemical composition of materials was determined by inductive plasma-coupled AES. For this, the loss of ignition of samples was determined. The silica-aluminas were dissolved by treating them with hydrofluoric acid (40 wt%) in Teflon-lined autoclaves in a microwave oven.

N_2 adsorption

The textural properties, the specific surface area, specific pore volume, and mean pore size and pore size distribution, were controlled by nitrogen adsorption and desorption measurements at the temperature of liquid nitrogen. The measurements were carried out on ASAP 2010 automatic sorption systems. Before measurements, the samples were dehydrated at 50 °C under vacuum for 12 h.

TEM

Images were investigated on a Philips CM 20 microscope using a LaB_6 cathode. Samples were supported on Lacey-carbon.

NMR

^{27}Al NMR measurements were performed on a Bruker Avance 600 spectrometer (Bruker Biospin GmbH, Rheinstetten, Germany, $B_0 = 14.1$ T). Magic angle sample spinning (MAS) was carried out at room temperature. The spectra were measured at 156.4 MHz using a 4 mm MAS probe at 13 kHz MAS spinning frequency speed for single pulse experiments. The repetition time was 2 s in all the cases. ^{27}Al chemical shifts (δ) were referenced using narrow AlO_6 signal of YAG set to $\delta = 0.6$ ppm. ^{29}Si NMR measurements were performed on a Bruker DMX 400 spectrometer at 79.46 MHz. The spectra were collected at 6.5 kHz MAS spinning frequency using a 7-mm MAS probe. For silica-alumina with 70 wt% SiO_2, 12 scans were sufficient to acquire with a repetition time of 1800 s. The corresponding numbers for the other samples were silica-alumina with 40 wt% SiO_2 900 s and 64 scans, silica-alumina with 20 wt% SiO_2: 1800 s and 128 scans, silica-alumina with 5 wt% SiO_2: 300 s and 488 scans. The ^{29}Si chemical shifts (δ) have been referenced using the Q signal of Q8M8 at $\delta = -109.6$ ppm. Furthermore, cross polarization (CP) experiments were performed. The ^{1}H 90° pulse length of 4.75 μs, a contact time of $\delta_{cp} = 2$ ms, and repetition time of 2 s were used for these CP measurements. A total of 1024 scans was accumulated for the sample with the highest silicate content (silica-alumina with 70 wt% SiO_2), whereas a 4 k scan was taken for silica-alumina with 5 wt% SiO_2. During the contact time, the silicon spin lock field strength was held constant, while the proton spin lock field was ramped linearly (ramp-CP) down to 50% of the initial value [12]. Proton decoupling was carried out with a 15° two-pulse phase modulation (TPPM) sequence [13].

FTIR

Measurements of ammonia were studied using an in situ IR cell using self-supporting silica-alumna discs. Before exposing to ammonia, samples were evacuated at elevated temperature to remove loosely bound water. Desorption of ammonia was followed by the decrease of characteristic

vibration bands of the adsorbed ammonia during continuous heating of the wafer up to 350 °C.

Ammonia-TPD

Measurements were carried on an AutoChem 2910 (Micromeritics) apparatus that was coupled with a mass spectrometer to differentiate between ammonia and water desorption. Approximately, 100 mg of the sample was activated in flowing helium at elevated temperature. After cooling down, the sample was contacted with ammonia diluted in helium at 110 °C and flashed with the carrier gas. Thereafter, the TPD run was carried out with a heating rate of 10 K up to a temperature of 350 °C.

Catalytic testing

The acetalization of benzaldehyde with butadiol-1,3 is sensitive to Brønsted acidity. Therefore, silica-alumina catalysts were not calcined and added to the reaction mixture in the hydrated form to prevent the loss of sites from dehydroxylation. Nearly stoichiometric amounts of the benzaldehyde and butanediol-1,3 were mixed into toluene. The total amount of starting materials was ca. 20 wt%. In addition, trimethylbenzene was added as an internal standard. The reaction mixture and 1 g of catalyst were given into the catalytic setup (glass apparatus) and was rapidly heated to ca. 110 °C by stirring under reflux. Water was removed by using a bypass. Small aliquots of reaction mixtures were used for GC–MS analysis.

Results and discussion

Textural characterization

XRD pattern confirms that mesoporous silica-aluminas derived from hydrolysis and co-precipitation from solutions containing organic silicon and aluminum precursors are X-ray amorphous. The TEM images show that silica-alumina consist of aggregated and/or interconnected nanosized particles (Fig. 1). They form an open porous network with large interstitial voids of some nanometer size.

Detailed textural data were derived from nitrogen adsorption measurements. The size maxima of the mesopores are located at ca. 8–10 nm with a broad distribution, indicating irregularity of the pore system for precipitated silica-aluminas and small pore size distribution for the ordered mesoporous aluminosilicate obtained by the addition of a template.

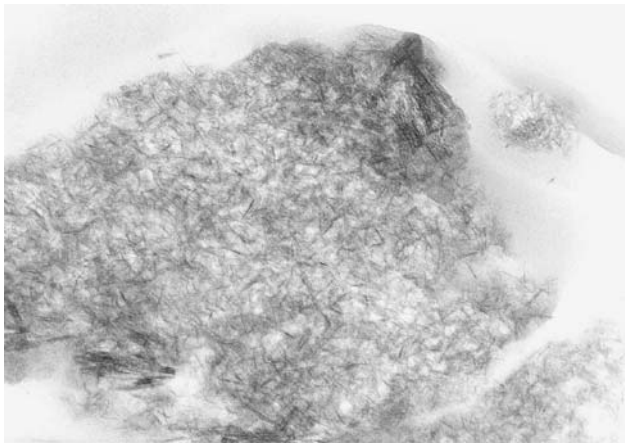

Fig. 1 TEM images of a representative silica-alumina sample showing the presence of irregular mesoporosity

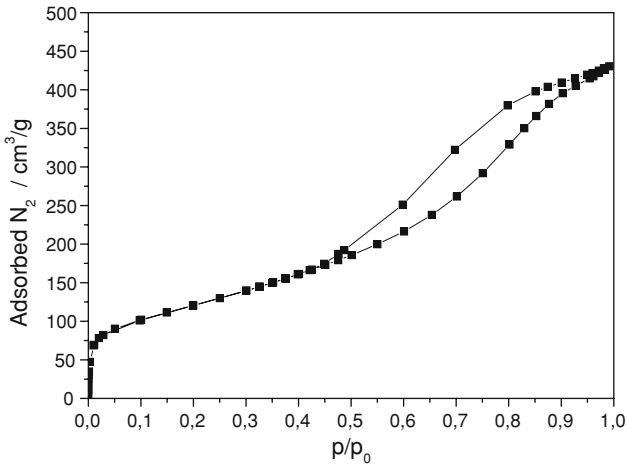

Fig. 2 Nitrogen adsorption–desorption isotherm of silica-alumina containing 20 wt% of silica

Observed nitrogen adsorption–desorption isotherms of silica-aluminas (Fig. 2) belong to the type IV according to the IUPAC nomenclature [14]. This type of curvature is typically observed with mesoporous materials. Starting at low p/p_0, a steep increase of the adsorption isotherm was observed. In the first adsorption stage, up to a relative nitrogen pressure of $p/p_0 = 0.2$, monolayer adsorption occurred at the pore walls. The further slow increase of the isotherm at increasing relative nitrogen pressure was due to multilayer adsorption. Between $p/p_0 = 0.5$ to 0.9, a second uptake step was observed. This uptake is due to capillary condensation in large mesopores. Micropores were detected.

The pore volumes of considered materials varied between 0.5 and 1 cm^3/g. BET surface areas exceed a range between 400 and 600 m^2/g. The mean pore sizes of amorphous silica-alumina range from 3 to 8 nm (Fig. 3) with a broad distribution, indicating irregularity of the pore system for co-precipitated silica-aluminas. The pores are

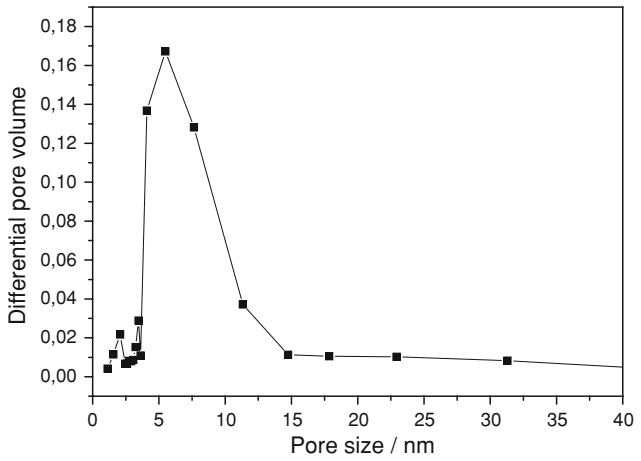

Fig. 3 Pore size distribution of silica-aluminas containing 20 wt% of silica

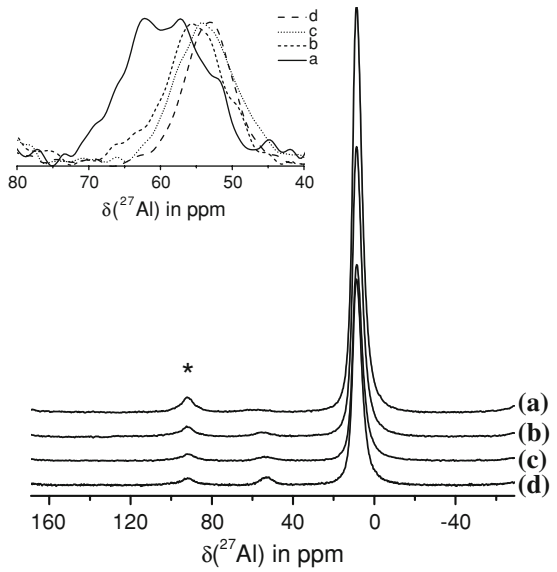

Fig. 4 ^{27}Al MAS NMR spectra of silica-aluminas with 5 (a), 20 (b, c) and 70 wt% SiO_2 (d), MAS spinning sidebands marked by asterisks; insert top left: expanded region of AlO_4 signals (normalized to each other), for details see text

Table 1 Textural data of silica-aluminas having different silica content

Sample	Specific pore volume (cm^3/g)	Mean pore size (nm)	BET surface area (m^2/g)
Silica-alumina 1.5 wt% SiO_2	0.43	4.5	348
Silica-alumina 5 wt% SiO_2	0.63	3.5; 5[a]	383
Silica-alumina 20 wt% SiO_2	0.65	5	435
Silica-alumina 40 wt% SiO_2	1.0	8	520

[a] Shoulder in the pore size distribution curve at the 3.5 nm maximum

markedly larger than those of ordered mesostructured materials with usual pore sizes of 0.3–1 nm. Textural data of silica-alumina obtained by nitrogen sorption measurements are given in Table 1.

With growing silica content, the specific pore volume, mean pore size, and specific surface areas increases. This finding is in agreement with the known network-forming ability of silica. It increases with growing SiO_2 content, as indicated by the textural data. Indeed, in contrast to alumina, e.g., pseudo-boehmite, which is expected to form the amorphous alumina phase, silica tends to form a three-dimensional network promoting the formation of porous materials.

Structural properties

An interesting feature of the silica aluminas represents the local environment of the aluminum sites, especially the coordination. The ^{27}Al MAS NMR spectra (cf. Fig. 4) of the amorphous silica-alumina sample show two signals, one dominating signal with a peak at 9 ppm, and a second, very weak one at about 55 ppm. These two signals are caused by octahedral- and tetrahedral- coordinated Al species, respectively. The strong octahedral site is typical for boehmite. Obviously, two tetrahedral AlO_4 sites are present in silica-alumina with 5 wt% SiO_2 as shown in Fig. 4 (insert top left: one at 64 ppm and another at about 59 ppm). With increasing silicate content, the AlO_4 signal at 64 ppm disappears and the 59 ppm signal shifts high field. The 64 ppm signal can presumably be assigned to AlO_4 units connected to octahedral AlO_6, whereas for higher silicate content and the observed high-field shift, the second site may be attributed to AlO_4 sites connected to SiO_4 groups.

The relative amount of AlO_4 sites with respect to the total aluminum can be obtained easily by integrating the spectra areas of the corresponding lines. The appearance of tetrahedral Al is closely related to the presence of silica and, generally, increases with growing SiO_2 content. Mean values obtained by three independent integrations are given in Table 2. As seen from this table, most of the aluminum is still present in boehmite as AlO_6 species; only very small number of tetrahedral AlO_4 sites is formed. This AlO_4 content can now be recalculated to yield the tetrahedral Al content in the silica-alumina sample and the apparent Si/Al ratio of the silicate phase, assuming that all the tetrahedral Al sites are connected to silica and the Loewenstein rule holds [15]. As shown in Fig. 5, it is obvious that for increasing silicate content, the AlO_4 reaches a maximum at 20% silicate content. There is a general agreement that these tetrahedral Al sites (Al_{tetr}) form Brønsted acid

Table 2 Composition, relative intensities of ^{27}Al NMR lines and apparent Si/Al ratios in silica-aluminas

SiO_2 content wt%	Rel. intensity of tetrahedral Al signal at 53 ppm (%)	Rel. intensity of octahedral Al signal at 9 ppm (%)	Content of Al_{tetr} expressed as AlOOH (wt%)	Si/Al ratio of aluminosilicate phase[a]
1.5	0.058	99.04	0.058	(26)
5	0.99	99.01	0.94	5.3
10	1.07	98.93	0.96	10.4
20	2.28	97.72	1.82	11
40	1.93	98.07	1.45	28
70	3.94	96.06	1.17	60

[a] Assuming that the tetrahedral coordinated aluminum is connected to the silicate

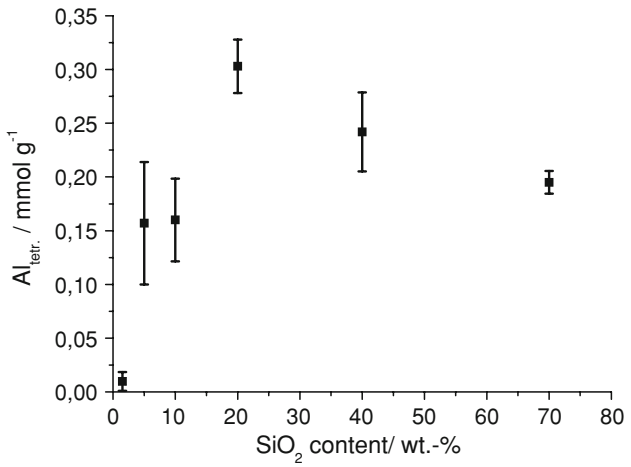

Fig. 5 Influence of the silica content on the concentration of tetrahedral Al in silica-aluminas

Al–O(H)–Si– bridges in porous silicate frameworks. Therefore, the concentration of Brønsted sites should follow the same trend as found with the tetrahedral aluminum (Table 2).

At higher silica content, the concentration of Al_{tetr} and, hence, Bronsted sites decreases again, although the relative amount of Al_{tetr} with respect to the octahedral Al (Al_{oct}) in still increasing. However, at high silica content, the absolute amount of alumina decreases markedly, thereby overcompensating the relative increase of Al_{tetr}. At the same time, the Si/Al ratio in the silicate phase increases. The catalytic consequence is a decrease of the Brønsted site concentration which is accompanied by an increase in the acidic strength due to the higher Si/Al ratio. The growing connectivity in the silicate framework additionally stabilizes (Brønsted acidic) the bridging hydroxyl groups against dehydroxylation.

The nature of silica was studied by ^{29}Si MAS and CPMAS NMR with 5, 20, 40, and 70 wt% SiO_2 plotted in Fig. 6. For the lowest silica content of 5%, an asymmetric line shape with a peak position of about −80 ppm is found with a pronounced low-field shoulder. Most interestingly, the CPMAS spectrum reproduces this spectrum completely within the limits of the signal-to-noise ratio. On the contrary, the ^{29}Si MAS NMR spectrum of the sample with the highest silica content of 70% has the typical form of the condensed silicate network with dominating Q^4 units (−112 ppm), a strong Q^3 signal at −100 ppm (one OH^- per Q unit), and some Q^2 sites (two silanol groups per Q site). This conclusion is not only based on the observed chemical shifts of the signals, but also on the CPMAS spectrum. It shows a strong peak for Q^3 and enhanced Q^2 signal intensity, while the Q^4 signal is weaker. All other spectra of Fig. 6 show the structural evolution in the samples if more and more silicate is incorporated. The higher the silicate content, the more the spectra show the presence of a silicate network. From that point of view, it is essential to understand the ^{29}Si spectrum of silica-alumina with 5 wt% SiO_2, which has the lowest silicate content of all the samples measured by ^{29}Si NMR. The peak position of −80 ppm can be interpreted in terms of boundary structures in two ways: either it describes a depolymerized silicate network consisting of Q^2 and Q^1 units or an aluminosilicate network consisting mainly of AlO_4(4Si) units which are known to display such ^{29}Si shifts [16].

The fact that the CPMAS spectrum is the same as the MAS NMR line shape hints stringently on the interpretation of silicate network. However, the stronger argument comes from the ^{27}Al MAS NMR spectrum. Given that all the Si of silica-alumina with 5 wt% SiO_2 (equivalent to 0.833 mmol/g) would form an aluminosilicate network, about 20% of the Al sites must be in tetrahedral configurations. This, however, can be completely ruled out, as only 0.157 mmol/g AlO_4 sites are present.

Catalysis

Ammonia-TPD measurements of silica aluminas show a broad, non-structured desorption peak between 150 and 400 °C. The desorption maximum is located near 200 °C. Maximum amount of ammonia is desorbed between 200 and 300 °C. These results show the presence of weak to

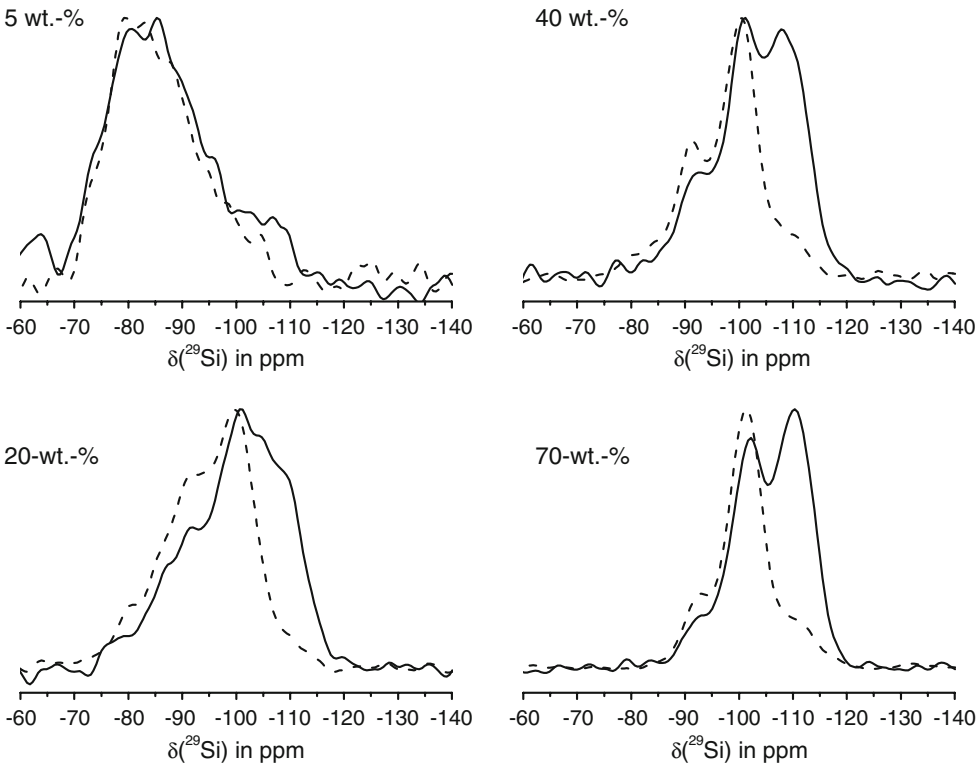

Fig. 6 ^{29}Si NMR spectra of the silica-aluminas with different SiO_2 content as indicated in the figure: solid lines: ^{29}Si MAS NMR spectra; hatched lines: ^{29}Si CPMAS NMR spectra

medium strong acid sites in non-dehydroxylated silica-aluminas. Above a temperature of 300 °C, measurements might by distorted by starting dehydroxylation of the material. The amount of acid sites increases with the silicon content and reaches its maximum at 20 wt% SiO_2. The maximum total amount of Brønsted and Lewis sites was ca. 0.5 mmol/g. Taking into account that this sample contains 0.3 mmol/g of Brønsted sites (compare Table 2), the difference of 0.2 mmol/g should belong to Lewis sites.

In addition, ammonia-FTIR measurements have been carried out to characterize the Brønsted acidity. FTIR spectra following the thermal desorption of ammonia are shown in Fig. 7. The absorption band at ca. 1450 cm^{-1} belongs to a characteristic mode of the formed protonated ammonium ion. The band intensity decreases rapidly with rising temperature (r.t. and 150 °C, respectively), in accordance with the results of the ammonia-TPD measurements. However, these samples contain also quantitative amounts of weak to medium strong Brønsted sites, which desorb ammonia between 200 and 300 °C.

The precipitated silica-aluminas are active and highly selective catalysts in the Bronsted acid-catalyzed acetalization in liquid-phase batch reactions. Nearly complete conversion with >95% selectivity to the acetal has been observed for all catalysts with exception of the very low silica content sample. This feature is an independent and strong proof for the presence of quantitative amounts of Brønsted acid sites in silica-aluminas and confirms NMR

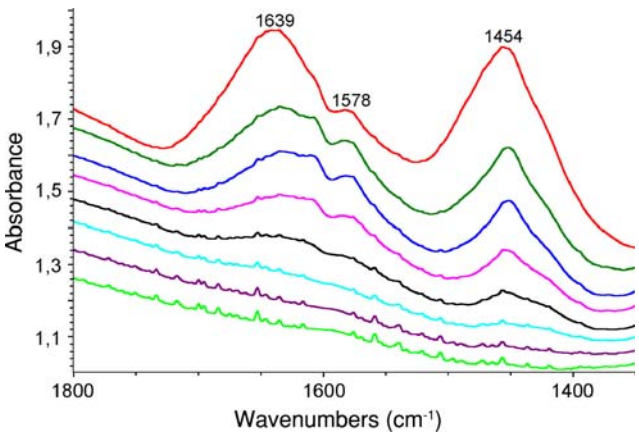

Fig. 7 FTIR-spectra of ammonia adsorbed on silica-aluminas containing 5 wt% of silica at different temperatures: r.t., 100 °C, 150 °C, 200 °C, 250 °C, 300 °C, 350 °C, and 400 °C from top to bottom

and TPD results presented above. In general, the reaction of the alcohol with the aldehyde starts very rapidly with high onset conversion. This period of relatively fast conversion continues for about 5 h. Thereafter, conversion proceeds slower as indicated by the different slops of conversion versus time on stream (Fig. 8). An explanation could be the competitive adsorption or the presence of the formed acetal in the pores of the catalysts. Partial filling of pores by the formed reaction product can inhibit the access of starting molecules to the catalytic surface as well as block some Brønsted sites. As mentioned above,

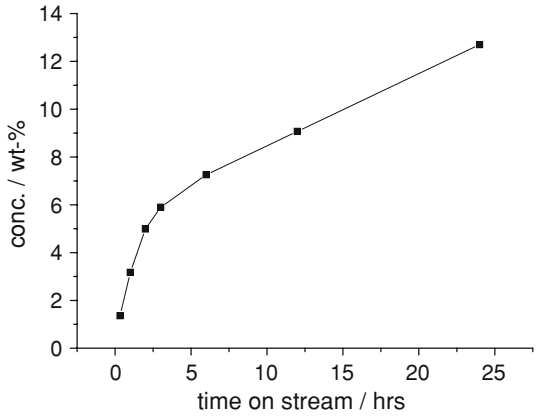

Fig. 8 Acetalization of benzaldehyde with butanediol-1,3 using a silica-alumina catalyst containing 10% of silica at 120 °C. Acetal formation versus time on stream

by-products are observed only to a very low extent. The GC–MS analysis showed the formation of benzylalcohol (usually <1 wt%). The silica-alumina catalysts could be removed by filtration. The washed and re-hydrated catalyst could be re-used.

The reaction proceeds at the Brønsted sites. Samples free of silica were not active. Also, calcined silica-aluminas are not active in this reaction. The presence of Brønsted sites is correlated with the silica content as illustrated by the onset conversion found with different silica-aluminas shown in Fig. 9. According to their catalytic activity, silica-aluminas can be divided into two groups: (i) lower active silica catalysts with $\leq$10 wt% of SiO_2 and (ii) higher active catalysts with >10 wt% SiO_2. The low silica catalysts show a moderate increase in the catalytic activity (conversion) with growing SiO_2 content, whereas higher silica catalysts are distinctly more active. They show a

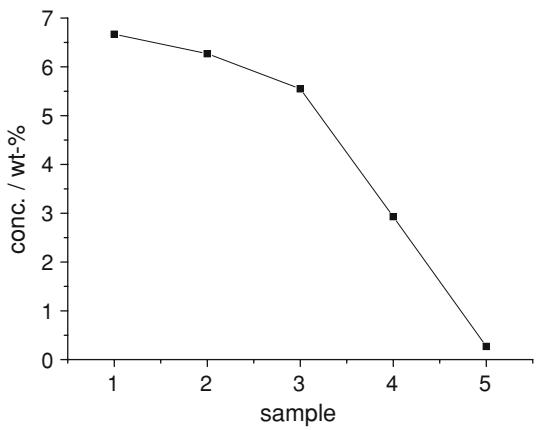

Fig. 9 Acetalisation of benzaldehyde with butanediol-1,3 using silica-alumina catalysts of different silica content: Change of the butanediol-1,3 content due to acetal formation. Reaction condition:: 120 °C, 20 min time on stream. 1—2 wt%, 2—5 wt%, 3—10 wt%, 4—20 wt% and 5—40 wt% of silica

steep increase in conversion with growing SiO_2 content. This is due to the fact that these samples contain lower amounts of Brønsted sites and a lower Si/Al ratio and framework connectivity, giving rise to low acidic strength of sites. In contrast, highly active catalysts contain higher amounts of Brønsted sites. However, this alone cannot explain the large differences in catalytic activity alone. More interestingly, these materials contain higher connected aluminosilicates combined with markedly higher Si/Al ratios (Table 2). The acidic strength is known to increase with growing Si/Al ratio [17–20]. The acidic strength is further improved by growing connectivity of the aluminosilicate framework. Content of silanol groups is decreased, and the framework electronegativity is enhanced. The influence of both effects, the amount and strength of sites, are illustrated by comparison of the catalytic activity of silica-alumina with 10 wt% SiO_2 (sample 3 in Fig. 9) with those of samples containing 20 and 70 wt% SiO_2 (sample 4 and 5 in Fig. 9). The increase in the conversion between samples 3 and 4 is mainly caused by the higher site concentration which nearly doubled from 0.16 to 0.3 mmol/g, respectively, whereas the Si/Al ratio of both samples (10.4 and 11) is nearly the same. In contrast, the large increase in the catalytic activity of sample 5 compared to sample 3 is strongly influenced by the acidic strength of Brønsted sites. Indeed, the Si/Al ratio increases from 10.4 to 60, whereas the amount of acid sites increases only moderately by 22% from 0.16 to 0.195 mmol/g.

Conclusion

In summary, combined investigations of textural, structural, acidity, and catalytic properties display the following: (i) Silica-aluminas are Brønsted acidic. The development of acidity is connected with the presence of tetrahedral aluminum in the silicate compartment. The appearance of tetrahedral Al sites is closely related to the presence of silica. The relative amount of tetrahedral Al sites increases with growing SiO_2 content with respect to the total Al content. However, the dependence of the concentration of tetrahedral Al in the samples on the SiO_2 content follows a volcano shape. It increases with growing SiO_2 content, reaches a maximum at ca. 20 wt% of silica, and decreases again with further growing of SiO_2. The reason behind this is the marked decrease of total alumina in samples with high silica content. It overcompensates the growth of the relative part of tetrahedral Al with respect to the total Al. However, in contrast to the volcano shape course of tetrahedral Al concentration, which correlates with Brønsted site concentration, the catalytic activity increases with growing SiO_2 content and shows a marked increase at high silica content. This is due to the interplay of acid site concentration and the

acidic strength. The latter is distinctly increased with high Si/Al ratio and silicate framework connectivity. Last but not the least, the network-forming ability of silica supports the formation of highly porous and surface-rich silica-alumina required for liquid-phase catalysis. (ii) ^{29}Si NMR spectra display only the silicate network connectivity. Si(Al)n units were not distinguished. The network polymerizes more and more with increasing silica content. This process is obviously continuous across the samples. On the contrary, the ^{27}Al MAS NMR spectra confirm both that boehmite is the dominating aluminate phase and that only very little amorphous aluminosilicate is formed. However, its concentration can be obtained as a function of the composition of the samples, and it is shown that it reaches a maximum for about 20% silicate content. (iii) Silica-aluminas are sufficiently active in proton acid catalyzed reactions, e.g., for use in fine chemical synthesis in solution under mild thermal condition. (iv) The performance of catalysts is improved by the superior textural properties. High-specific surface area combined with high porosity and large mesopore size allows easy access also of larger molecules to the active sites. (v) The nature of silicate compartment determines the catalytic and textural properties. The controlled preparation of aluminosilicate compartments is a key factor for the preparation of amorphous silica-alumina with improved properties.

Acknowledgement The authors thank Dr. M.-M. Pohl for recording the TEM image. The excellent assistance from Dr. U. Bentrup and Mrs. M. Halle in FTIR and ICP measurements is gratefully acknowledged.

References

1. Khaleel AA, Klabunde KJ (2002) Chem Eur J 8:3991
2. Yurdakovic M, Akcay M, Toubul Y, Yurdakovic K (1999) Turk J Chem 23:319
3. Xu M, Lunsford JH, Goodman DW, Bhattacharyya A (1997) Appl Catal A 149:289
4. Bourne KH, Cannings FR, Pitkethly RC (1970) J Phys Chem 71:2197
5. Tanabe K, Hölderich W (1999) Appl Catal A 181:399
6. Bevilacqua Montanari MT, Finocchio E, Busca G (2006) Catal Today 116:132
7. Danielle W, Schubert U, Glöckler R, Meyer A, Noweck K, Knözinger KH (2000) Appl Catal A 196:399
8. Crépeau G, Montouillout V, Vimont A, Mariey L, Cseri T, Maugé F (2006) J Phys Chem B 110:15172
9. Hunger M, Freude D, Pfeifer H, Bremer H, Jank M, Wendlandt KP (1983) Chem Phys Lett 100:29
10. Rouxhet PG, Scokart PO, Canesson P, Defossé C, Rodrique L, Declerck FD, Leonard AJ, Delmon B, Damon JP (1976) In: Kerker M (ed) Colloid and interface science, vol 3. Academic Press, New York, p 81
11. Sârbu C, Delmon B (1999) Appl Catal A 185:85
12. Metz G, Wu XL, Smith SO (1994) J Magn Reson A 110:219
13. Bennett E, Rienstra CM, Auger M, Lakshmi KV, Griffin RF (1995) J Chem Phys 103:6951
14. IUPAC Reporting physorption data for gas/solid systems (1985) Pure Appl Chem 57:603
15. Loewenstein W (1954) Am Mineral 39:92
16. Engelhardt G, Koller H (1994) In: Diehl P, Fluck E, Günter H, Kosfeld R, Seelig J (eds) NMR basic principles and progress. Springer Verlag, Berlin, p 1
17. Stach H, Jänchen J, Lohse U (1992) Catal Lett 13:9
18. Mortier WJ (1978) J Catal 55:138
19. Barthmeuf D (1987) Mater Chem Phys 17:64
20. Barthomeuf D (1994) Zeolites 14:394